Desalination and Water Treatment
www.deswater.com

doi: 10.1080/19443994.2015.1095127

57 (2016) 19051–19061
September

Taylor & Francis
Taylor & Francis Group

Role of hygroscopic triethylene glycol and relative humidity in controlling morphology of polyethersulfone ultrafiltration membrane

P.C. Tan, S.C. Low*

School of Chemical Engineering, Engineering Campus, Universiti Sains Malaysia, Seri Ampangan, 14300 Nibong Tebal, Pulau Pinang, Malaysia, email: peng_chee91@hotmail.com (P.C. Tan), Tel. +604 5996412; Fax: +604 5941013; emails: chsclow@usm.my, siewchun@gmail.com (S.C. Low)

Received 16 April 2015; Accepted 13 September 2015

ABSTRACT

This article presents the physical microstructure and chemical properties of polyethersulfone (PES) ultrafiltration membranes, dedicated to comprehend the role of hygroscopic triethylene glycol (TEG) under controlled conditions of relative humidity and membrane's exposure time before immersion in the coagulation bath. The pore characteristics and chemical properties of the resulting membranes were studied by coupling the scanning electron microscopy sectional images with capillary flow porometer, porosity measurement and Fourier transform infrared spectroscopy. Separation capabilities of membranes were examined through filtration tests using humic acid solution as the model system. The remarkably high performance of the PES ultrafiltration membrane in humic acid removal was mainly attributed to the hygroscopic TEG that retained water molecules during dry phase inversion, which produced membranes with high porosity. However, excessive absorption of water vapour by either high concentration of TEG or humid condition led to a low productivity membrane due to the formation of dense skin structure at the membrane's uppermost layer. In the present work, 10 min of membrane's exposure time in humid environment with 25 wt.% TEG in casting dope and relative humidity of 60% was managed to fabricate a membrane with a thin selective top layer and finger-like substructure, leading to a high productivity of 145 L/m^2 h and 95% humic acid rejection.

Keywords: Hygroscopic; Relative humidity; Phase inversion; Morphology; Ultrafiltration

1. Introduction

Polyethersulfone (PES) membranes have long been pursued to improve filtration efficiency for water treatment [1–3] due to the good thermal stability of polymer, high mechanical strength and excellent resistance to chemicals such as bases, acids and hydrocarbons even at high temperatures [4,5]. The wide operating temperature and pH make PES polymer a pioneer polymer to be employed in membrane technology for potable water production with reliable effluent quality. Nevertheless, membrane fouling caused by the hydrophobic characteristic of the PES polymer remains a critical issue in the water filtration processes and is the dominant factor that restricts its widespread applications [6,7].

In general, hydrophilic membranes exhibit lower level of fouling with higher flux reversibility at the membrane surface [8]. Hence, the addition of

*Corresponding author.

hydrophilic additives is a common practice to enhance membrane hydrophilicity [4,9–11]. Nevertheless, the use of additives implies in a more complex system due to the existence of a fourth component, that will change the phase equilibrium and overall mass transfer rate. Therefore, further investigation into membrane phase inversion is needed to control the membrane final morphology and properties.

Phase inversion is based on bringing a homogeneous polymer solution to become thermodynamically unstable to initiate the mass transfer process. For instance, a combination of the dry and wet phase inversion techniques has been discussed for slower mass transfer processes [12–15]. The casted film is induced in humid air (dry phase inversion) prior to immersion in a liquid coagulation bath (wet phase inversion) [16]. Indeed, the rapidity of the dry phase inversion could be regulated by adding hygroscopic additives into the casting dope [17]. The hygroscopic additives, such as triethylene glycol (TEG) [18], possess the tendency to absorb water vapour from the surrounding and hence induce a thermodynamically unstable system for a faster phase inversion. Consequently, a membrane with a bigger pore structure is expected.

In dry phase inversion, the level of relative humidity was found significantly affecting the membrane morphology [13,19] particularly in cases where water is a strong non-solvent for the polymer [19]. During phase inversion, the initial casted dope is in contact with the humid surrounding where higher relative humidity will enhance the driving force for the net diffusion and promote the absorption of water molecules into the solution-casted film. At a longer exposure time, the hygroscopic TEG contained in the solution-casted film will absorb more water vapour, leading to a highly porous membrane [20,21]. By controlling the evaporation time as well as the humid environment, it is possible to control the skin thickness of the membrane.

This article presents the physical microstructure and chemical properties of PES membranes, dedicated to comprehend the role of hygroscopic TEG under controlled conditions of relative humidity and exposure time. In view of the prominent role of water vapour intake by casting dope during dry phase inversion in defining membrane final structure, the concentration of hygroscopic TEG as well as relative humidity and exposure time to the humid environment were investigated. The hygroscopic TEG was expected not only to enhance the hydrophilicity of the PES membrane, but also help in adjusting the membrane morphology through the combined dry–wet phase inversion. The changes in the membrane physical microstructures and chemical properties were further related to its performances in terms of flux and rejection of humic acid.

2. Materials and methods

2.1. Materials

Polyethersulfone (PES Ultrason E6020P with M_w = 58,000 Da) was supplied by BASF company (Germany). The solvent, N-methylpyrrolidone (NMP), and hygroscopic additive, triethylene glycol (TEG) were purchased from Merck (Germany) and Acros Organics (Belgium), respectively. Humic acid, HA (Sigma-Aldrich, USA), and calcium chloride (R & M Marketing, UK) were used as the organic foulant. 1 M HCl (Merck, Germany) and 1 M NaOH (Merck, Germany) were used for pH adjustment. All the chemicals were used as received without further purification.

2.2. Membrane synthesis

13 wt.% of PES polymer was dissolved in NMP solvent at a temperature of 40˚C and a stirring speed of 700 rpm. Hygroscopic TEG (ranging from 0 to 50 wt.%) was then added into the casting dope and continuously stirred for 3 h until a homogeneous clear solution was obtained. The casting dope was then degassed to remove air bubbles. Subsequently, the casting dope was casted onto a glass plate with a 250 μm clearance gap of casting blade in a humidity controllable glove box. The solution-casted film was then exposed to dry phase inversion at specific relative humidity (ranging from 35 to 85%) for a preset exposure time (ranging from 0 to 10 min). The detailed membrane formulation and casting conditions are tabulated in Table 1. The casted film was then immersed into the distilled water coagulation bath for 20 h to further induce wet phase inversion to remove the residual solvent.

2.3. Membrane characterization

2.3.1. Field emission scanning electron microscopy (FESEM)

Surface morphology and cross-sectional structure of PES membranes were observed using scanning electron microscopy (Hitachi TM 3000, Japan). For membrane cross-sectional structure, the sample was immersed in the liquid nitrogen and cryogenically cracked. All membrane samples were coated with a thin conducting layer (gold/palladium (Au/Pd)) to prevent sample charging by accumulation of static electric fields.

Table 1
Membrane formulation and process parameters for each experimental run

Membrane	PES concentration (wt.%)	NMP concentration (wt.%)	TEG concentration (wt.%)	Relative humidity (%)	Duration of vapour-induced phase inversion (min)
Run 1	13	62	25	60	10
Run 2	13	62	25	85	5
Run 3	13	37	50	60	5
Run 4	13	62	25	60	0
Run 5	13	87	0	60	5
Run 6	13	62	25	60	5
Run 7	13	62	25	35	5

2.3.2. Pore characteristics

The mean through pore diameter and the pore size distribution of membrane were determined using liquid–liquid displacement porometer (Porolux 1000, Germany). Through pore diameter is referring to the smallest constriction part along the pore channel and therefore determines the effective pore functionality. Prior to porometer testing, the membrane was first immersed in the perfluoroether (porefil liquid) with a surface tension of 16 dynes/cm and is thoroughly wetted for 5 min. The gas flow was measured as a function of transmembrane pressure, first through the wet membrane with perfluoroether (wet curve) and then through the dry membrane (dry curve) [22]. During measurement, the pressure of inert gas N_2 was increased gradually; there will be no gas flow through the pores until capillary forces have been overcome, releasing liquid from the pore. The pressure was increased continuously until all wetting liquid was purged out from the membrane sample. Thereafter, there was complete gas flow which equals to the gas flow through a dry membrane. The relationship between the pore size and the corresponding pressure was calculated based on the Young–Laplace equation.

To determine the membrane's porosity, the sample was cut into dimensions of 1 cm × 1 cm and the thickness was measured. The initial weight of the membrane was recorded as W_1. The membrane sample was then dried in oven for 20 min at 40°C. The weight of the dried sample was then recorded as W_2. The heating and weighing processes were repeated until a constant value of W_2 was obtained. The porosity of the membrane was then calculated using Eq. (1):

$$P\ (\%) = \frac{(V_a - V_e)}{V_a} \times 100\% \quad (1)$$

where V_a = apparent volume (cm^3) = membrane surface area × membrane thickness and V_e = existence volume (cm^3) = W_2 (g)/ρ_{PES} (g/cm^3), where ρ_{PES} is the density of PES.

2.3.3. Attenuated total reflectance-Fourier transform infrared spectroscopy (ATR-FTIR)

The presence of TEG within the membrane matrix was analysed using Thermo Scientific Fourier transform infrared spectrometer (ATR-FTIR, NICOLET iS10, USA) over the wavenumber range of 4,000–525 cm^{-1}. Diamond crystal was used with an incident angle of 45°. Each spectrum resulted from 16 scans with a resolution of 4 cm^{-1}.

2.3.4. Thermogravimetric analysis (TGA)

Thermogravimetric analyser (Perkin–Elmer TGA 7, USA) was utilized to find out the existence of TEG in the casted film as well as to assess thermal stability of the as-cast membrane. The heating profile was set to increase from room temperature to 650°C at a ramping rate of 10°C/min in nitrogen atmosphere with a purge rate of 20 mL/min.

2.4. Evaluation of membrane performances

The membrane performances were evaluated in terms of permeation flux and humic acid (HA) rejection. 5 ppm HA aqueous solution and 1 mmol/L calcium chloride were used as feed solutions. Calcium chloride was used to adjust the ionic strength of the HA solution. The pH level of the feed solution was maintained at 7 by adding 1 M hydrochloric acid. Filtration test was conducted using a dead-end stirred cell (model 8050, Millipore Corp., Bedford, MA) with an effective membrane area of 12.57 cm^2 connected to an ultrapure grade nitrogen-pressurized reservoir. All the filtration tests were performed at a pressure of 1 bar at a constant agitation speed of 350 rpm to

minimize concentration polarization. Accumulated permeate mass was read by a computer-recorded electronic balance (FX3000i AND, USA); these data would later be used to calculate the filtration flux (J). The concentration of HA in the permeate was evaluated using UV–vis spectrophotometer (Pharo 300 Spectroquant, Merck Millipore) by measuring absorbance at 254 nm. All filtrations were carried out in few replicates and the average filtration results were reported.

The permeation flux of the humic acid solution was calculated as follows:

$$J = \frac{\Delta W}{\rho A \Delta t} \tag{2}$$

where J is the permeation flux (L/m^2 h), ΔW (g) is the collected permeate during the sampling time, A is the effective membrane area (m^2), ρ is the density of water (g/L) and Δt is the sampling time (h).

The rejection of humic acid was calculated as:

$$R\ (\%) = \left(1 - \frac{C_p}{C_f}\right) \times 100\% \tag{3}$$

where R is the rejection (%), C_p is the humic acid concentration in the permeate (ppm) and C_f is the humic acid concentration in feed stream (ppm).

3. Result and discussion

Firstly, the concentration effect of TEG was investigated. Casting dopes containing TEG with 0, 25 and 50 wt.% were studied, while dry phase inversion exposure time was set constant at 5 min at a relative humidity level of 60%. Fig. 1 demonstrates the surface and cross-sectional morphology of the synthesized membranes. As clearly seen in Fig. 1, the membrane pore morphology was highly relying on the TEG content in the casting dope. Smaller membrane pores (Fig. 1(a), 0.026 μm) were observed when no TEG was added to the casting dope. The absence of hygroscopic TEG in the casted film induced a relatively slow dry phase inversion process and thereby resulted in smaller surface pores. In contrast, the pore size of the membrane casted with a TEG content of 50 wt.% (Fig. 1(c), 0.583 μm) was 22 times larger than that of the neat PES membrane (Fig. 1(a)). This confirmed the aggressive hygroscopic role of TEG and its pore-forming role in changing the final membrane structure. At a higher content of TEG, more moisture was absorbed by the hygroscopic TEG into the casted film. With increased water content in the casted film, homogeneity of the polymer matrix was greatly decreased due to the low solubility of PES polymer in water compared to NMP. Finally, it brought the thermodynamically unstable solution-casted film closer to the region of liquid–liquid phase separation, which resulted in bigger pores on the membrane top layer.

Macrovoid finger-like cross-sectional structure was formed in the neat PES membrane (Fig. 1(a)) when TEG was excluded. As more TEG was added into the casting solution (Fig. 1(b), 25 wt.% TEG and Fig. 1(c), 50 wt.% TEG), viscosity of the casting dopes was increased gradually. In fact, the viscous solution will slow down the inter-diffusion rate between the solvent (NMP) and the non-solvent (water molecules from the coagulation bath) during wet phase inversion. Under this condition, the PES polymer did not have enough time to phase separate, where the internal layer of the solution-casted film would then be solidified by the inflow of water molecules. Thus, it suppressed the asymmetric finger-like growth, as observed in Fig. 1(c). This observation is in accordance with the research outcome by Idris et al. [23], who found a narrower finger-like structure when the viscosity of the dope solution was increased by the addition of polyethylene glycol.

A similar porosity of 83% was obtained for the neat PES membrane (Fig. 1(a)) and the PES membrane casted with 25 wt.% TEG (Fig. 1(b)) attributed to the finger-like cross-sectional structures. As for the membrane casted with a higher content of TEG (50 wt.%), the membrane's porosity was reduced to 61 ± 3% with a thinner film thickness of 64 ± 4 μm. As discussed, this was due to the rapid dry phase inversion through the excessive absorption of humid air by the hygroscopic TEG. As such, the content of TEG needs to be controlled in order to maintain the high flux finger-like structure with governable surface pore morphology.

Intermolecular interactions between TEG and PES polymer were investigated by the ATR-FTIR technique. In Fig. 2(a), the spectrum of the pure hygroscopic TEG shows a broad stretching O–H and C–H vibrating band at 3,400 and 2,900 cm^{-1}, respectively. The strong peak at 1,250–1,000 cm^{-1} was associated with the bending vibration of the aliphatic chain of the C–O–C bond. Besides, the spectral bands of the pure PES membrane (Fig. 2(b)) showed a sharp peak at 1,580 cm^{-1}, ascertained to the stretching frequency of the C–H bond from the benzene ring. The aromatic C=C stretching bond and the aromatic ether bond from the PES polymer were found at 1,480 and 1,250 cm^{-1}. Two strong peaks at 1,150 and 1,100 cm^{-1} were referred to the stretching frequencies of the SO_2 group of PES. By comparing all three components

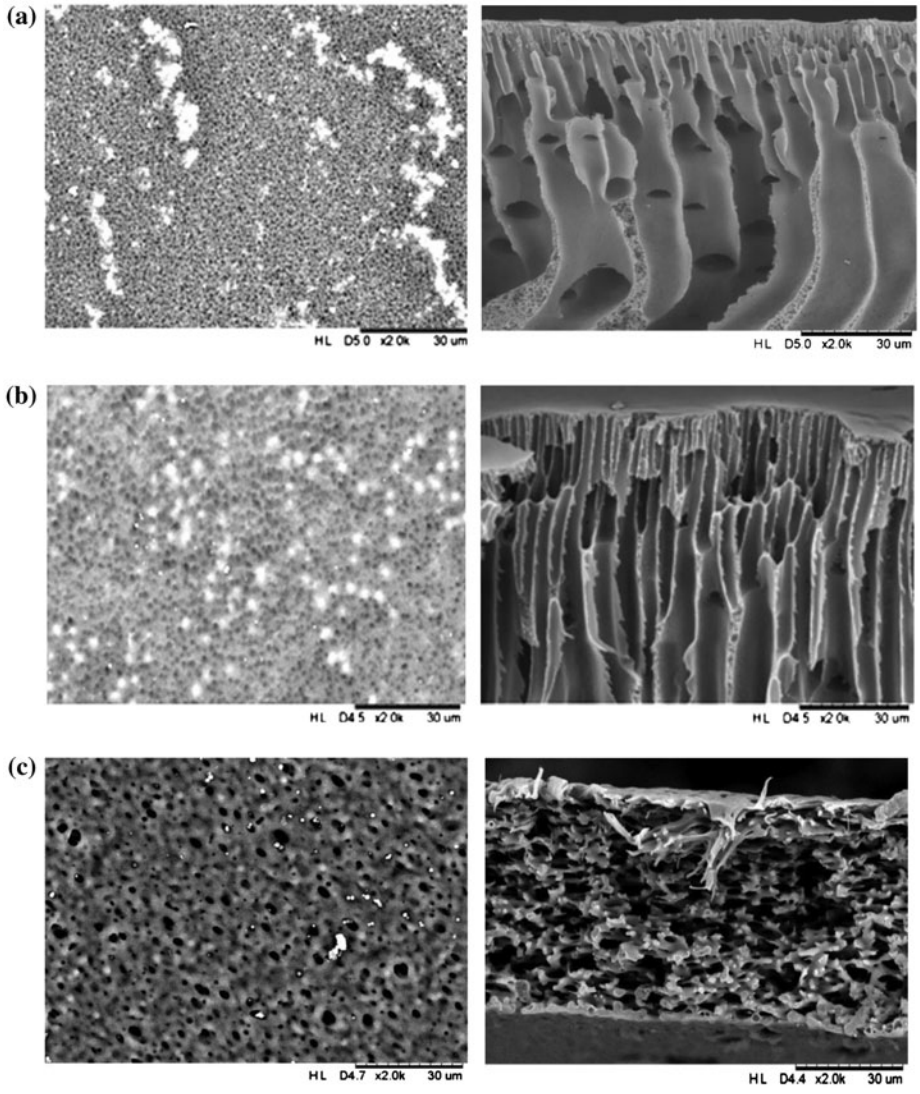

Fig. 1. Surface (left) and cross-sectional (right) micrographs of membrane synthesized at: (a) 0 wt.%, (b) 25 wt.% and (c) 50 wt.% TEG added as the hygroscopic agent in the casting dope (membranes casted at RH = 60% and 5 min of vapour-induced phase inversion).

(pure TEG, neat PES membrane and PES–TEG membrane), no characteristic peaks of TEG were seen in the PES–TEG casted film. This indicates that all TEG was eventually diffused out from the polymer film during the wet phase immersion precipitation process.

The existence of TEG in the casted film was further assessed through thermogravimetric analysis (TGA). Due to the highly hygroscopic role of TEG with a superior water absorption capability, the pure TEG demonstrated considerable weight loss (18%) before 100˚C, attributed to the removal of absorbed water vapour (Fig. 3). The onset of TEG degradation occurred around 120˚C. With TEG boiling point of 285˚C, no residual remained after high temperature combustion at 650˚C. On the other hand, both membranes casted with 25 and 50 wt.% TEG illustrated no significant weight loss until 500˚C. Decomposition of the PES polymer backbone was initiated at temperatures of 510 and 525˚C for casted film with 25 and 50 wt.% TEG, respectively. This indicated that PES membranes possess sufficiently high thermal stability for industrial application in wastewater treatment. Based on the insignificant weight loss recorded at a temperature of 120˚C, it could be concluded that all TEG had diffused out from the casted membrane during wet phase inversion, which was in accordance with the FTIR result.

Thus, in addition to the hygroscopic role of TEG during initial dry phase inversion, TEG also acted as the pore former as in the latter wet phase immersion

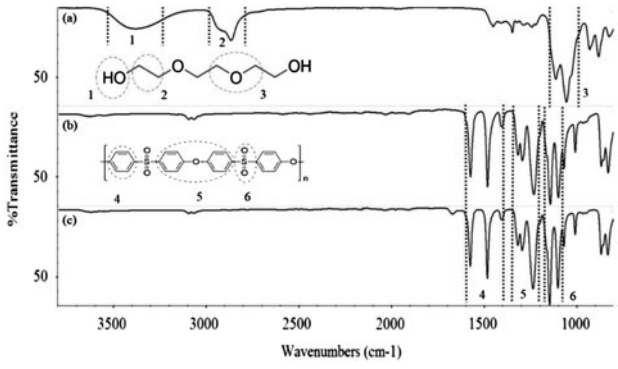

Fig. 2. FTIR spectra of: (a) pure TEG, (b) neat PES membrane and (c) PES–TEG membrane (casted with 25 wt.% TEG and 5 min of vapour-induced phase inversion at a relative humidity of 60%).

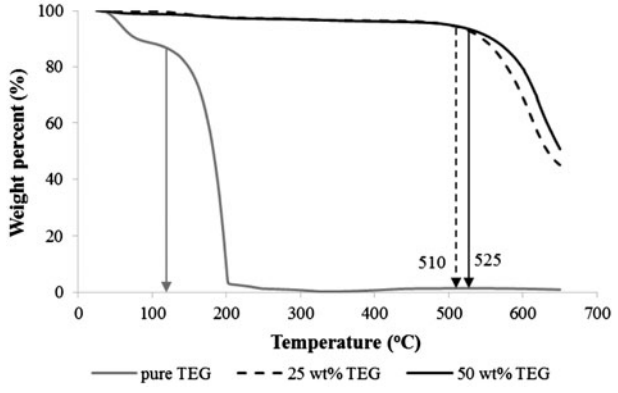

Fig. 3. TGA thermograms for pure TEG and membranes casted at different TEG concentrations (at RH = 60% and 5 min of dry phase inversion).

precipitation process, which contributed to the highly porous finger-like membrane structure. These results were in accordance to the SEM micrographs in Fig. 1, where bigger pore structures were formed when a higher content of TEG was added to the casting dope. However, the over-added amount of TEG (50 wt.%) may defeat the purpose of TEG as pore former, which caused adverse effect to the membrane morphology. As seen from Fig. 1(c), a spongy cross-sectional structure was observed instead of the finger-like structure when 50 wt.% TEG was incorporated. The membrane cross-sectional structure is mainly governed by two factors: (i) the role of TEG as pore former which resulted in finger-like structure and (ii) viscosity of the casting dope. At an excessively high TEG concentration (50 wt.%), the highly viscous casting dope plays a dominant role in determining the membrane cross-sectional structure. Indeed, the high viscous solution will slow down the overall wet phase inversion that restricts effective polymer phase separation. Hence, a spongy structure was observed instead of the asymmetric finger-like structure.

As expected, the membrane performed at a lower flux (Fig. 4) when no TEG was added to the casting dope, attributed to the smaller pore structures (Fig. 1(a), 0.026 μm). As discussed earlier, the membrane structure was evolved by the existence of TEG in the casting dope by which the thermodynamic state of the polymer solution was altered to achieve phase inversion. Creation of larger effective pores was favoured by the hygroscopic TEG that absorbed more water vapour, on par with the enhancement of permeate flux for membrane casted with 25 wt.% TEG. The membrane exhibited three times higher steady flux (33 L/m^2 h) as compared to the neat PES membrane. The further increased concentration of TEG in the casting dope (50 wt.% TEG) had demonstrated a low flux productivity (steady flux at 10 L/m^2 h), although bigger membrane pores were created by the presence of the hygroscopic TEG. This result seems to be counter-intuitive as, in general, a bigger pore structure contributes to a higher flux. It can be explained by the membrane morphology via SEM micrograph. The compact and rigid porous structures (Fig. 1(c), 50 wt.% TEG) offered greater transport resistance and hence restricted the passage of water molecules across the membrane thickness, leading to a low flux performance. This result indicated the close interrelation between hygroscopic TEG and phase inversion behaviour in controlling the membrane microstructure for separation capability.

As discussed, the incorporation of hygroscopic TEG into the casting dope dominated the rate of water sorption to achieve a better control of membrane morphology. In view of that, the level of relative humidity (available amount of water vapour) and the exposure time during dry phase inversion (duration allocated

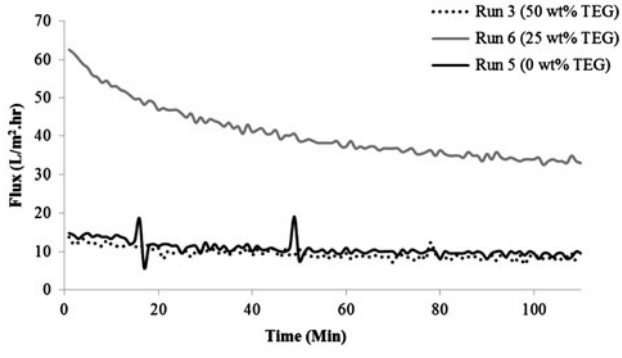

Fig. 4. Flux performances for membrane synthesized at different TEG concentrations (casted at RH = 60% and 5 min of vapour-induced phase inversion).

for water vapour sorption) are two main interrelated factors that affect water sorption by TEG. Hence, it is worth to interrelate the hygroscopic role of TEG to the controlled environment (relative humidity and exposure time in dry phase inversion) on the final microstructure of the membrane.

Based on the pore characteristics results from porometer, the prolonged exposure time to the humid environment (25 wt.% TEG and relative humidity of 60%) had generated a smaller surface pore structure to the PES membrane, which decreased from 0.024 μm (5 min of exposure time) to 0.018 μm (10 min of exposure time). The result was in accordance to the previous discussion. The longer the membrane was in contact with the humid air, the more the water vapour penetrated into the membrane matrix and hence initiated nucleation, which resulted in membrane solidification. With a longer exposure time, polymer stood a higher chance to agglomerate to the uppermost layer prior to getting subjected to the rapid wet phase immersion precipitation. Once agglomeration occurred, the connection between the polymer matrices tended to be closer, creating smaller surface pores. In contrast, at 0 min of exposure time (membrane casted without dry phase inversion), the wet phase immersion precipitation process demonstrated a bigger pore size (0.28 μm), which was 15 times bigger as compared to the membrane that underwent 10 min of dry phase inversion (0.018 μm). In wet phase inversion, the mass exchange rate between the solvent (NMP) and the non-solvent (liquid water) occurred rapidly as the membrane was surrounded by the coagulation water bath. The rapid diffusion of water into the membrane induced spontaneous liquid–liquid demixing where a bigger pore size was expected. By incorporating dry phase inversion, the overall phase inversion promoted slower solvent–non-solvent mass transfer rate, whereby water vapour was slowly absorbed by the hygroscopic TEG through the membrane top surface [12], leading to a membrane microstructure with a smaller pore size.

Surprisingly, a similar finger-like structure was obtained over the studied range of exposure time (Fig. 5). However, a thin layer of spongy structure was observed when a longer exposure time was applied (Fig. 5(c)). As seen, the membrane cross-section could be divided into two portions. Generally, the membranes that were exposed to 0 min (Fig. 5(a)) and 5 min (Fig. 5(b)) of the humid environment had demonstrated a narrower finger-like structure at the region of portion A compared to the region of portion B. During dry phase inversion, water vapour penetrated into the membrane sub-layer to promote nucleation where polymer agglomeration occurred.

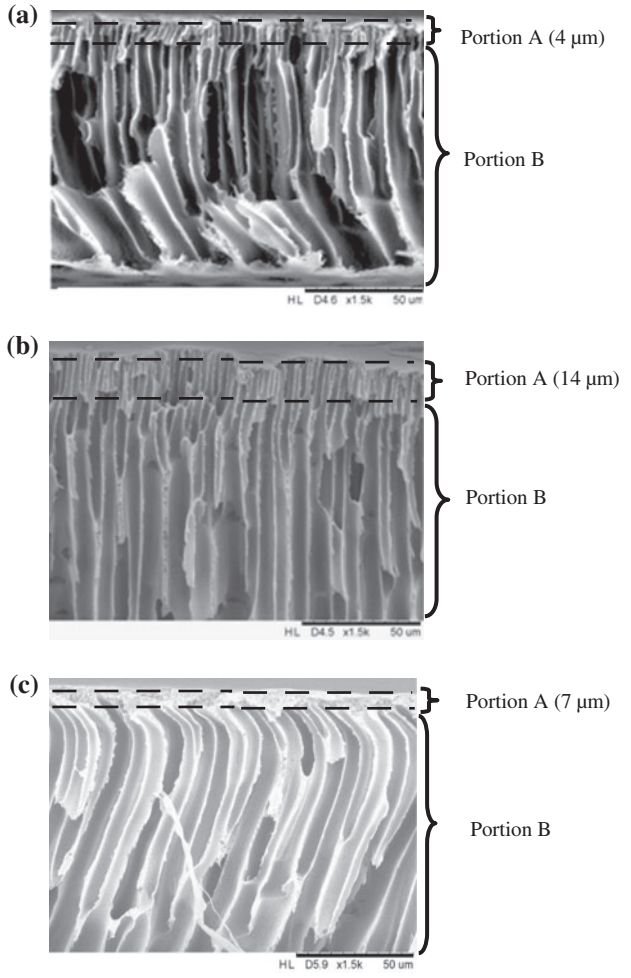

Fig. 5. Cross-sectional micrographs of membrane that underwent (a) 0 min, (b) 5 min and (c) 10 min of exposure time during dry phase inversion (membrane casted at a TEG concentration of 25 wt.% and RH = 60%).

Consequently, a membrane layer with a lower porosity and narrower finger-like structure resulted, as shown in the portion A (Fig. 5(a) and (b)). As in region A, membrane that was exposed to 5 min of humid atmosphere had a thicker narrower finger-like structure as compared to that of 0 min, with a thickness of 14 and 4 μm, respectively. The thicker and narrower finger-like structure was formed due to the prolonged exposure time that allowed deeper diffusion of water vapour into the polymer matrix prior to wet immersion precipitation. On the other hand, a 7 μm dense spongy layer was found in the membrane that underwent 10 min of dry phase inversion (Fig. 5(c)). It was believed that the longer exposure time of membrane during dry phase inversion will promote serious nucleation at the membrane–air interface. Hence, a denser microstructure at region A was observed.

A wider finger-like structure was observed in region B for all three membrane samples. At this region, less humid vapour could diffuse towards the deeper layer across the membrane thickness, thus delaying the nucleation process over portion B and causing a broader finger-like structure. Similar porosities were observed for each membrane prepared at different durations of dry phase inversion, ranging from 82 ± 1% to 83 ± 0.8% due to the analogous finger-like structure. A similar result was also reported by Li et al. where a longer exposure time will only affect the surface microstructure at the membrane–air interface [21].

From separation performance tests, the membrane that underwent immersion precipitation without dry phase inversion (0 min of exposure time) recorded a higher steady permeation flux at 130 L/m^2 h, as displayed in Fig. 6. The high productivity achieved was mainly contributed by its bigger membrane pores. Interestingly, the membrane that was exposed to 10 min of humid environment (with a 7 μm denser spongy layer at membrane–air interface) performed a similar high flux at 145 L/m^2 h. The high fluxes were mainly attributed to the high membrane porosity (around 83% for both membrane) and the broad finger-like structure at the sub-layer region B (Fig. 5(a) and (c)). In contrast, the membrane that underwent 5 min of dry phase inversion which also consisted of a broad finger-like structure at region B (Fig. 5(b)) had demonstrated a lower flux performance (33 L/m^2 h). It is believed that a greater transport resistance of the thicker portion A (14 μm narrower finger-like structure) had restricted the motion of feed solution across the membrane, despite both membranes exhibiting a similar high porosity at 83%. The role of membrane dense skin thickness in affecting permeation flux had also been discussed by Yip et al. where a higher permeation flux was observed in a thinner and more porous thin-film composite forward osmosis (TFC FO) membrane [24].

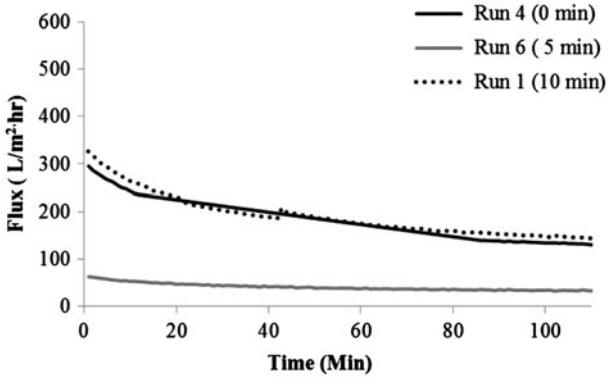

Fig. 6. Flux performances for membrane casted at different durations of vapour-induced phase inversion with a TEG concentration of 25 wt.% and 60% relative humidity.

Membrane rejection performance mainly depends on the membrane structure at the polymer–air interface that restricts the transport of solute across the membrane. The membrane that underwent longer vapour-induced phase inversion (10 min) undoubtedly demonstrated the highest humic acid rejection at 95% due to its dense skin layer that restricted the passage of humic substances. Although the membrane that underwent an immediate immersion precipitation without dry phase inversion (0 min of dry phase exposure time) possessed a similar high flux as that exposed to 10 min of humid environment; a 31% decrease in humic acid rejection was recorded. This means some humic substances were still able to pass through the narrower finger-like structure (Fig. 5(a)). In this regard, a combination of dry–wet phase inversion was preferable in controlling and tailoring the membrane morphology to optimize membrane performances in terms of productivity and separation efficiency.

Since the exposure time in humid environment possesses significant effects on the microstructure of the membrane, two extreme humid conditions at dry state (RH at 35%) and wet state (RH at 85%) were also carried out in this work. Smaller surface pores were observed when the membrane was casted under the highly humid condition (RH at 85%) at 0.017 μm, as compared to previous 0.024 μm when the RH was preset at 60%. In some embodiments, the hydrophobic PES polymer restricted the absorption of humid molecules and did not allow the water to enter or fill the membrane's pores. Although hygroscopic TEG was introduced into the casted film, the repulsion of some humid molecules away from the hydrophobic PES membrane surface was a spontaneous process, leading to slower water vapour diffusion into the membrane internal layer. In turn, water vapour accumulated on the surface of the casted film.

Evidence of this water repulsion phenomenon by the hydrophobic PES membrane is illustrated in Fig. 7. A compact spongy cross-sectional structure with a 20 μm dense skin formation was observed when an extremely high relative humidity (85%) was applied in dry phase inversion. As mentioned above, the faster solidification process attributed to the high accumulation of water vapour at the membrane uppermost layer induced a more serious nucleation. Thus, PES polymer had a higher opportunity to agglomerate at the membrane top surface that led to the formation of the dense skin layer. The dense skin layer further limited diffusion of water vapour into membrane internal

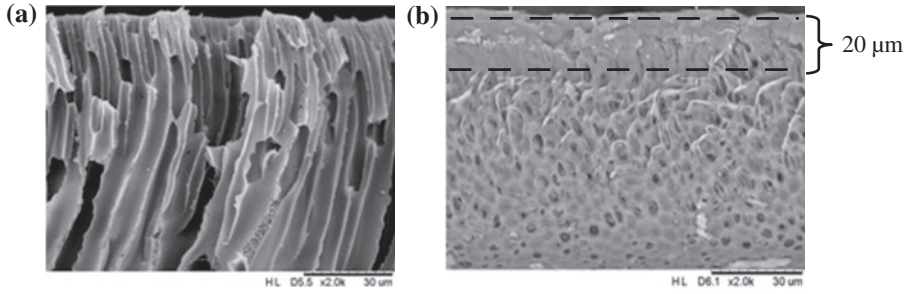

Fig. 7. Cross-sectional micrograph of membrane casted at: (a) 35% and (b) 85% relative humidity (membrane casted at a TEG concentration of 25 wt.% and 5 min of vapour-induced phase inversion).

layer, promoting a slow demixing process which resulted in a spongy structure (Fig. 7(b)).

On the other hand, a dry environment (RH at 35%) promoted a similar finger-like cross-sectional structure as the membrane casted at a RH of 60%, with relatively bigger surface pores at 0.027 μm. A straight and through pore channels observed in the SEM micrograph (Fig. 7(a)) indicated the minimal accumulation of humid vapour on the membrane surface. A higher flux was expected for the straight through pore channel at the expense of lower humic acid rejection performance. Filtration test can help verify this hypothesis as well as lead to an improved understanding of the physical humid environment necessary for better filtration performances. It has been generally accepted that membrane productivity is closely related to the membrane pore size [25]. Fig. 8 reveals that the permeation flux of the membrane synthesized at a relative humidity of 35% recorded the highest flux (45 L/m^2 h). As mentioned above, it was simply due to the bigger surface pores and straight finger-like pore channels found in the membrane synthesized under dry atmosphere (0.027 μm). However, increasing water flux is usually accompanied by decreased rejection property in the membrane. Only 77% humid

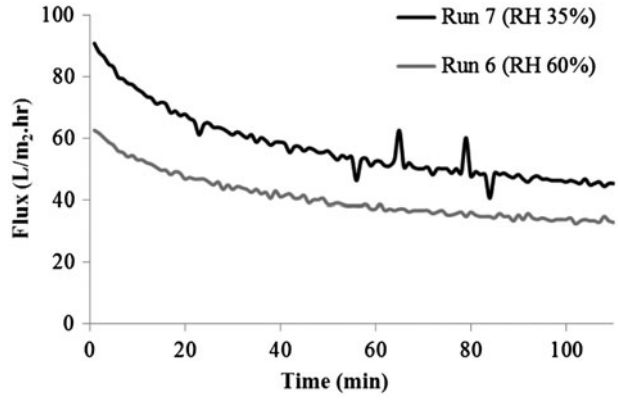

Fig. 8. Flux performance of membrane casted at different relative humidities and at a TEG concentration of 25 wt.% and 5 min of vapour-induced phase inversion.

acid rejection was recorded. On the other hand, no permeation flux was being collected for the membrane casted under wet condition with a relative humidity of 85%. The dense skin layer and compact cross-sectional structure formed (Fig. 7(b)) was expected to create a large resistance for the transport of water molecules through the membrane; as such no permeate was collected at a transmembrane pressure of

Table 2
Summary for membrane characterization and performance

Membrane	TEG concentration (wt.%)	Relative humidity (%)	Duration of vapour-induced phase inversion (min)	Porosity (%)	Pore size (μm)	Steady-state flux (L/m^2 h)	Humic acid rejection (%)
Run 1	25	60	10	83 ± 0.8	0.018	145	95
Run 2	25	85	5	79 ± 0.7	0.017	0	NA[a]
Run 3	50	60	5	61 ± 3	0.583	7	96
Run 4	25	60	0	82 ± 1	0.280	130	64
Run 5	0	60	5	83 ± 0.5	0.026	10	74
Run 6	25	60	5	83 ± 0.4	0.024	33	77
Run 7	25	35	5	82 ± 0.8	0.027	45	67

[a]Rejection cannot be determined; no permeation flux was being collected.

1 bar. The characterizations and performances of each membrane are summarized in Table 2.

Among the membranes synthesized, the Run 1 membrane demonstrated the best separation performances with a permeation flux of 145 L/m^2 h and a humic acid rejection at 95%. As a comparison to the research carried out by Qin et al., the hollow fibre PES membrane corresponded to the permeation flux of 16.7 L/m^2 h at 1 bar transmembrane pressure with 97.9% humic acid rejection [26]. Although the Run 1 membrane in the present work has demonstrated 2.9% lower humic acid rejection, its 10 times higher permeation promises superior practicability in large-scale wastewater treatment. At 3 bar of transmembrane pressure, PES membranes synthesized by Mehrparvar et al. illustrated 79% humic acid rejection and 33 L/m^2 h permeation flux [27], which is four times lower than that in the present work although the membrane performed at a higher operating pressure. Besides, a permeation flux of 25 L/m^2 h and 88% humic acid rejection were also reported by the same group when gallic acid was added to the PES membrane [27]. In comparison to a similar research on humic acid removal by PES membranes, the Run 1 membrane synthesized in the present work has showed not only a higher steady-state flux (at least four times higher) but also an excellent humic acid rejection.

4. Conclusion

This paper presents the theoretical and experimental study of humidity control and the hygroscopic role of TEG in controlling the microstructure of ultrafiltration PES membranes. By combining the interrelated hygroscopic role of TEG in absorbing humid vapour, effects of relative humidity and the dry phase exposure time, the membrane prepared with a casting dope composition of PES/NMP/TEG = 13/62/25 (wt.%), 10 min of exposure time and relative humidity of 60% demonstrated the best membrane separation performances, with a permeation flux of 145 L/m^2 h and 95% HA rejection. TEG was found as an absorbent in dry phase inversion to absorb water vapour from the humid air, and pore former in latter immersion precipitation process by creating a higher membrane porosity. However, excessive absorption of water vapour by either a high TEG content, or a highly humid condition led to a low productivity membrane due to the dense skin formation and compact spongy structure at the membrane's uppermost layer. An evolution from finger-like structure to spongy structure could be observed by controlling the three parameters (content of TEG, level of relative humidity and the exposure time) precisely. With a combination of 10 min dry phase inversion and latter immersion precipitation (wet phase), a porous top layer with a finger-like sub-layer resulted, leading to a membrane with a good permeation flux and HA rejection performances. In this regard, a combination of dry–wet phase inversion was recommended to control membrane morphology in a systematic manner and hence optimize membrane performances.

Acknowledgement

The authors wish to acknowledge the financial support granted by Universiti Sains Malaysia Research University (RU) Grant (1,001/PJKIMIA/814,230). All authors are affiliated to the Membrane Science and Technology Cluster of USM.

Nomenclature

A	—	effective membrane area (m^2)
C_f	—	humic acid concentration in feed stream (ppm)
C_P	—	humic acid concentration in permeate (ppm)
J	—	permeation flux (L/m^2 h)
P	—	porosity percentage (%)
R	—	rejection percentage (%)
V_a	—	apparent volume (cm^3)
V_e	—	existence volume (cm^3)
W_1	—	initial weight of membrane before drying (g)
W_2	—	final weight of membrane after drying (g)
Δt	—	sampling time for filtration test (h)
ΔW	—	collected permeate during the sampling time (g)
ρ	—	density of water (g/L)
ρ_{PES}	—	density of PES polymer (g/cm^3)

References

[1] H. Zhou, D.W. Smith, Advanced technologies in water and wastewater treatment, J. Environ. Eng. Sci. 1 (2002) 247–264.

[2] L.L. Hwang, H.H. Tseng, J.C. Chen, Fabrication of polyphenylsulfone/polyetherimide blend membranes for ultrafiltration applications: The effects of blending ratio on membrane properties and humic acid removal performance, J. Membr. Sci. 384 (2011) 72–81.

[3] F. Ma, H. Ye, Y.Z. Zhang, X.L. Ding, L.G. Lin, L. Zhao, H. Li, The effect of polymer concentration and additives of cast solution on performance of polyethersulfone/sulfonated polysulfone blend nanofiltration membranes, Desalin. Water Treat. 52 (2014) 618–625.

[4] Y. Mansourpanah, A. Gheshlaghi, F. Rekabdar, Structural analysis of PES nanoporous membranes under different conditions of preparation, Desalin. Water Treat. 50 (2012) 302–309.

[5] J.J. Qin, M.H. Oo, Y. Li, Development of high flux polyethersulfone hollow fiber ultrafiltration membranes from a low critical solution temperature dope via hypochlorite treatment, J. Membr. Sci. 247 (2005) 137–142.

[6] H. Yu, Y. Zhang, J. Zhang, H. Zhang, J. Liu, Preparation and antibacterial property of SiO_2–Ag/PES hybrid ultrafiltration membranes, Desalin. Water Treat. 51 (2013) 3584–3590.
[7] A. Ahmad, A. Abdulkarim, S. Ismail, B. Ooi, Preparation and characterisation of PES-ZnO mixed matrix membranes for humic acid removal, Desalin. Water Treat. 54 (2015) 3257–3268.
[8] Q. Ng, J. Lim, A. Ahmad, B. Ooi, S. Low, Efficacy evaluation of the antifouling magnetite-PES composite membrane through QCM-D and magnetophoretic filtration performances, Sep. Purif. Technol. 132 (2014) 138–148.
[9] M. Amirilargani, M. Sadrzadeh, T. Mohammadi, Synthesis and characterization of polyethersulfone membranes, J. Polym. Res. 17 (2010) 363–377.
[10] B. Vatsha, J.C. Ngila, R.M. Moutloali, Preparation of antifouling polyvinylpyrrolidone (PVP 40 K) modified polyethersulfone (PES) ultrafiltration (UF) membrane for water purification, Phys. Chem. Earth, Parts A/B/C 67–69 (2014) 125–131.
[11] C. Liu, Y. Yun, N. Wu, Y. Hua, C. Li, Effects of amphiphilic additive Pluronic F127 on performance of poly (ether sulfone) ultrafiltration membrane, Desalin. Water Treat. 51 (2013) 3776–3785.
[12] D. Bouyer, W. Werapun, C. Pochat-Bohatier, A. Deratani, Morphological properties of membranes fabricated by VIPS process using PEI/NMP/water system: SEM analysis and mass transfer modelling, J. Membr. Sci. 349 (2010) 97–112.
[13] H. Sun, S. Liu, B. Ge, L. Xing, H. Chen, Cellulose nitrate membrane formation via phase separation induced by penetration of nonsolvent from vapor phase, J. Membr. Sci. 295 (2007) 2–10.
[14] P.K. Annamalai, C. Pochat-Bohatier, D. Bouyer, C.L. Li, A. Deratani, D.M. Wang, Kinetics of mass transfer during vapour-induced phase separation (VIPS) process and its influence on poly-(vinylidene fluoride) (PVDF) membrane structure and surface morphology, Desalin. Water Treat. 34 (2011) 204–210.
[15] H. Tsai, C. Kuo, J. Lin, D. Wang, A. Deratani, C. Pochat-Bohatier, K. Lee, J. Lai, Morphology control of polysulfone hollow fiber membranes via water vapor induced phase separation, J. Membr. Sci. 278 (2006) 390–400.
[16] W. Liu, Z. Zhao, L. Sun, M. Wang, Formation of polyethersulfone film with regular microporous structure by water vapor induced phase separation, Chin. J. Chem. Eng. 18 (2010) 529–532.
[17] H. Susanto, N. Stahra, M. Ulbricht, High performance polyethersulfone microfiltration membranes having high flux and stable hydrophilic property, J. Membr. Sci. 342 (2009) 153–164.
[18] J. Li, A. Ito, Dehumidification and humidification of air by surface-soaked liquid membrane module with triethylene glycol, J. Membr. Sci. 325 (2008) 1007–1012.
[19] H.C. Park, Y.P. Kim, H.Y. Kim, Y.S. Kang, Membrane formation by water vapor induced phase inversion, J. Membr. Sci. 156 (1999) 169–178.
[20] S.J. Shin, J.P. Kim, H.J. Kim, J.H. Jeon, B.R. Min, Preparation and characterization of polyethersulfone microfiltration membranes by a 2-methoxyethanol additive, Desalination 186 (2005) 1–10.
[21] J.F. Li, Z.L. Xu, H. Yang, Microporous polyethersulfone membranes prepared under the combined precipitation conditions with non-solvent additives, Polym. Adv. Technol. 19 (2008) 251–257.
[22] S. Low, A. Ahmad, N. Ideris, Q. Ng, Interaction of isothermal phase inversion and membrane formulation for pathogens detection in water, Bioresour. Technol. 113 (2012) 219–224.
[23] A. Idris, N. Mat Zain, M.Y. Noordin, Synthesis, characterization and performance of asymmetric polyethersulfone (PES) ultrafiltration membranes with polyethylene glycol of different molecular weights as additives, Desalination 207 (2007) 324–339.
[24] N.Y. Yip, A. Tiraferri, W.A. Phillip, J.D. Schiffman, M. Elimelech, High performance thin-film composite forward osmosis membrane, Environ. Sci. Technol. 44 (2010) 3812–3818.
[25] H. Yu, X. Zhang, Y. Zhang, J. Liu, H. Zhang, Development of a hydrophilic PES ultrafiltration membrane containing SiO_2@N-Halamine nanoparticles with both organic antifouling and antibacterial properties, Desalination 326 (2013) 69–76.
[26] J.J. Qin, Y.M. Cao, M.H. Oo, Preparation of poly(ether sulfone) hollow fiber UF membrane for removal of NOM, J. Appl. Polym. Sci. 99 (2006) 430–435.
[27] A. Mehrparvar, A. Rahimpour, M. Jahanshahi, Modified ultrafiltration membranes for humic acid removal, J. Taiwan Inst. Chem. Eng. 45 (2014) 275–282.